CrystEngComm

PAPER

View Article Online
View Journal | View Issue

Cite this: *CrystEngComm*, 2017, **19**, 5549

The impact of *N,N′*-ditopic ligand length and geometry on the structures of zinc-based mixed-linker metal–organic frameworks†

Andrew D. Burrows, *[a] Siobhan Chan,[a] William J. Gee, [ab] Mary F. Mahon,*[a] Christopher Richardson, [c] Viorica M. Sebestyen,[a] Domenyk Turski[a] and Mark R. Warren [d]

Combining $Zn(NO_3)_2 \cdot 6H_2O$ with a series of dicarboxylic acids in the presence of the *N,N′*-ditopic ligand di(4-pyridyl)-1*H*-pyrazole (Hdpp) results in a series of mixed-linker metal–organic frameworks (MOFs) that have been crystallographically characterised. The reaction with 1,4-benzenedicarboxylic acid (H_2bdc) gives $[Zn_2(bdc)_2(Hdpp)_2] \cdot 2DMF$ **1**, which shows $Zn_2(\mu\text{-carboxylate})_2(carboxylate)_2$ secondary building units (SBUs) linked by bdc ligands into sheets, and these are pillared by the Hdpp linkers into a doubly-interpenetrated three-dimensional network. The reaction with 1,4-naphthalene dicarboxylic acid (H_2ndc-1,4) gives two products: $[Zn_2(1,4\text{-ndc})_2(Hdpp)] \cdot 4DMF$ **2a** forms a three-dimensional network in which sheets, formed from $Zn_2(carboxylate)_4$ 'paddle-wheel' SBUs being linked by 1,4-ndc, are connected together by Hdpp pillars, whereas $[Zn(1,4\text{-ndc})(Hdpp)] \cdot DMF$ **2b** forms a fourfold interpenetrated structure based on diamondoid networks with single zinc centres as nodes. The reaction with 1,3-benzenedicarboxylic acid (H_2mbdc) produces $[Zn(mbdc)(Hdpp)] \cdot DMF$ **3**, which forms a two-dimensional network with (4,4) topology in which ZnO_2N_2 nodes are interlinked by mbdc and Hdpp linkers. The reaction with 5-methyl-1,3-benzenedicarboxylic acid (H_2mbdc-Me) also forms a two-dimensional network structure, $[Zn_2(mbdc\text{-}Me)_2(Hdpp)_2] \cdot DMF$ **4**, albeit wherein dicarboxylates bridge between zinc-dicarboxylate tapes, themselves formed by interlinking of $Zn_2(\mu\text{-carboxylate})_2(carboxylate)_2$ SBUs similar to those in **1**. Finally, the reaction with 2,6-naphthalene dicarboxylic acid (H_2ndc-2,6) yields two crystalline species, both having the formula $[Zn_2(2,6\text{-ndc})_2(Hdpp)] \cdot DMF$ **5a**/**5b** and possessing infinite zinc-carboxylate chain motifs interlinked by both naphthalene rings and Hdpp linkers into a three-dimensional framework. In compounds **1**, **2b**, **3** and **4**, the pyrazole NH groups are involved in hydrogen bonding that serves to link either interpenetrated networks or neighbouring sheets together. However, in **2a** and **5a**/**5b** the NH groups project into the pores of the framework enabling interactions with guest molecules.

Received 8th August 2017,
Accepted 12th September 2017

DOI: 10.1039/c7ce01447c

rsc.li/crystengcomm

Introduction

Over recent years there has been a rapid growth of interest in metal–organic framework (MOF) materials.[1] This has largely been driven by their potential for porosity, which affords access to a wide range of applications, including gas storage,[2] catalysis[3] and separations.[4]

Currently, there is intense interest in the introduction of chemical functionalities onto the linkers, as a means of tuning the properties of the resultant MOFs.[5] This can be achieved either by using functionalised linkers in the synthesis,[6] or by post-synthetic modification protocols.[7] Both approaches take advantage of the fact that many MOFs form isoreticular series[8] – MOFs that have the same structural topology, but differ in the length and/or functionalities on the linkers.

Many MOFs contain a combination of anionic polycarboxylate linkers and neutral polypyridine linkers. For example, $[Zn_2(bdc)_2(dabco)]$, DMOF-1 (bdc = 1,4-benzenedicarboxylate, dabco = 1,4-diazabicyclooctane),[9a] $[Zn_2(bdc)_2(bpy)]$ (bpy = 4,4′-bipyridine)[9b,10] and $[Zn(mbdc)(bpy)]$ (mbdc = 1,3-benzenedicarboxylate)[11] are all well studied

[a] *Department of Chemistry, University of Bath, Claverton Down, Bath BA2 7AY, UK. E-mail: a.d.burrows@bath.ac.uk*
[b] *School of Physical Sciences, University of Kent, Canterbury, Kent CT2 7NZ, UK*
[c] *School of Chemistry, Faculty of Science, Medicine and Health, University of Wollongong, Wollongong, NSW 2522, Australia*
[d] *Diamond Light Source, Harwell Science and Innovation Centre, Didcot, Oxon OX11 0DE, UK*

† Electronic supplementary information (ESI) available: CCDC: 1555058–1555064. For general experimental details, powder patterns for **1**–**5**, and crystallographic details. For ESI and crystallographic data in CIF or other electronic format see DOI: 10.1039/c7ce01447c

systems in which substitution of bdc or mbdc for a functionalised analogue has been demonstrated, and the resultant effects probed.[12]

In contrast to this, studies in which the neutral *N*,*N*′-donor has been replaced by a functionalised analogue are far less common. Hupp and co-workers have reported MOFs containing a number of functionalised *N*,*N*′-ditopic linkers including alkyne-containing *trans*-1,2-di(4-pyridyl)ethenes[13] and dipyridyl-substituted 1,4,5,8-naphthalenetetracarboxydiimide,[14] 1,2,4,5-tetrazine[15] and manganese-salen complexes.[16] They have also demonstrated a solvent-assisted ligand exchange in which a dipyridyl-functionalised ethanediol was replaced by bpy.[17] Suh and co-workers have introduced a bridging dipyridyl tetrazine into a MOF *via* a post-synthetic modification, whereas Boyd, James and co-workers reported a chiral analogue of bipy and used this to prepare zinc MOFs.[18]

We previously reported the synthesis of di(4-pyridyl)-1*H*-pyrazole (Hdpp), and showed how it reacts with zinc(II) acetate and zinc(II) chloride to form network structures.[19] Hdpp remains protonated throughout these reactions and, as a consequence, the counter-ions are included as terminal ligands in the structures, which in turn limits the dimensionality of the frameworks produced. The protonated pyrazole group contains both hydrogen bond donors and acceptors, and the hydrogen bonding competes with coordination bonding in the observed solid state crystal structures.

We reasoned that Hdpp had the potential to act in a similar manner to other neutral *N*,*N*′-ditopic ligands in polycarboxylate-containing MOFs. We therefore sought to investigate the effect of the longer linker length with respect to bpy and dabco on the network structures formed with zinc dicarboxylates. In addition, we reasoned that the central five-membered pyrazole ring in Hdpp would reduce the angle between the pyridyl nitrogen donors from 180° as observed in bpy and dabco to approximately 156°, and that this difference might also have structural consequences. Finally, it was anticipated that the presence of the hydrogen bond donor and acceptor on the pyrazole ring would provide the potential for the network to act as a selective host for guests containing complementary hydrogen bonding faces.

Experimental

General experimental details and the synthesis of Hdpp[20] are provided in the ESI.†

Synthesis of 1–5

[Zn_2(bdc)$_2$(Hdpp)$_2$]·2DMF 1. Hdpp (0.044 g, 0.20 mmol), $Zn(NO_3)_2{\cdot}6H_2O$ (0.119 g, 0.40 mmol) and H_2bdc (0.066 g, 0.40 mmol) were dissolved in 20 cm^3 of anhydrous DMF with gentle heating and stirring. The colourless solution was placed in a 40 cm^3 Ace pressure tube, sealed and heated at 120 °C for 2 days. The resultant colourless hexagonal crystals were separated by filtration and washed with fresh DMF. Yield 0.050 g (48%). The PXRD pattern of the sample matched that simulated from the X-ray single crystal structure (Fig. S1†). Anal. calcd. for $C_{48}H_{42}N_{10}O_{10}Zn_2$ (1049.68), **1**: C, 54.92; H, 4.03; and N, 13.34%. Found: C, 54.98; H, 4.14; and N, 13.40%. The single crystals were produced from a similar reaction using $ZnCl_2$ as the zinc(II) source.

[Zn_2(1,4-ndc)$_2$(Hdpp)]·4DMF 2a and [Zn(1,4-ndc)(Hdpp)]·DMF 2b. Hdpp (0.022 g, 0.10 mmol), 1,4-naphthalene dicarboxylic acid (0.043 g, 0.20 mmol) and $Zn(NO_3)_2{\cdot}6H_2O$ (0.027 g, 0.10 mmol) were dissolved in 6 cm^3 of anhydrous DMF with gentle stirring. The colourless solution was placed in a Biotage pressure vial, capped and heated at 130 °C for 2 days. The resultant colourless crystals were separated by filtration and washed with fresh DMF. Two different crystal structures (**2a** and **2b**) were obtained from these crystals, confirming that the sample was not phase-pure. This was further evidenced by the PXRD pattern, which showed the dominant species to be **2a** (Fig. S2†). Crystals of compound **2b** were observed to undergo a morphological change when removed from the reaction medium and exposed to air, as can be seen in Fig. S6.†

[Zn(mbdc)(Hdpp)]·DMF 3. Hdpp (0.111 g, 0.50 mmol), $Zn(NO_3)_2{\cdot}6H_2O$ (0.297 g, 1.00 mmol) and H_2mbdc (0.166 g, 1.00 mmol) were dissolved in 10 cm^3 anhydrous DMF with gentle heating and stirring. The colourless solution was placed in a 20 cm^3 Ace pressure tube, sealed and heated at 120 °C for 2 days. The colourless hexagonal crystals were separated by filtration and washed with fresh DMF. Yield 0.20 g (76%). The PXRD pattern of the sample matched that simulated from the X-ray single crystal structure (Fig. S4†). Anal. calcd. for $C_{22.5}H_{19.5}N_{4.5}O_{5.5}Zn$ (506.31), Zn(mbdc)(Hdpp)·H_2O·0.5DMF: C, 53.36; H, 3.87; N, 12.09%. Found: C, 53.38; H, 3.88; and N, 12.45%.

[Zn_2(mbdc-Me)$_2$(Hdpp)$_2$]·DMF 4. Hdpp (0.111 g, 0.50 mmol), $Zn(NO_3)_2{\cdot}6H_2O$ (0.297 g, 1.00 mmol) and 5-methylisophthalic acid (0.180 g, 1.00 mmol) were dissolved in 10 cm^3 anhydrous DMF with gentle heating and stirring. The resulted colourless solution was placed in a 20 cm^3 Ace pressure tube, sealed and heated at 120 °C for 24 h. The colourless block-shaped crystals were separated by filtration and washed with fresh DMF. Yield 0.11 g (44%). Anal. calcd. for $C_{47}H_{45}N_9O_{12}Zn_2$ (1058.69), **4**·3H_2O: C, 53.32; H, 4.28; N, 11.9%. Found: C, 53.20; H, 4.21; and N, 11.5%.

[Zn_2(2,6-ndc)$_2$(Hdpp)]·DMF 5a, b. Hdpp (0.022 g, 0.10 mmol), 2,6-naphthalene dicarboxylic acid (0.043 g, 0.20 mmol) and $Zn(NO_3)_2{\cdot}6H_2O$ (0.027 g, 0.1 mmol) were dissolved in 6 cm^3 anhydrous DMF with gentle stirring. The colourless solution was placed in a vial, capped and heated at 130 °C for 2 days. The resultant block-like pale yellow crystals showed signs of degradation at low temperatures during the course of collecting single crystal X-ray data, whereas collection at room temperature only gave poor resolution X-ray data. However, when the solvent was removed from the reaction vial and the crystals were left at room temperature for several weeks, a change in morphology was observed, resulting in crystals with better defined edges. Single crystal X-ray diffraction analysis revealed that two types of crystal were present with different unit cell parameters and space

groups (**5a** and **5b**), though both were shown to have the same gross structure. PXRD studies showed a reasonable match between the bulk sample and that simulated from the crystal structure of **5b** (Fig. S5†). Anal. calcd. for $C_{44.5}H_{41.5}N_{6.5}O_{11.5}Zn_2$ (982.12), 5·H_2O·1.5DMF: C, 54.42; H, 4.26; N, 9.27%. Found: C, 54.61; H, 3.96; and N, 9.31%.

Crystallography

The zinc compounds prepared in this study were all structurally characterised using single-crystal X-ray diffraction techniques. While full data have been provided in the ESI,† key data are summarised below:

Crystal data for $C_{96}H_{84}N_{20}O_{20}Zn_4$ (**1**): M = 2099.31 g mol^{-1}, orthorhombic, space group $P2_12_12_1$ (no. 19), a = 16.5520(2), b = 18.8640(2), c = 29.4330(3) Å, U = 9190.07(17) Å^3, Z = 4, T = 150 K, μ(MoK$_\alpha$) = 1.116 mm^{-1}, D_{calc} = 1.517 g cm^{-3}, 125 929 reflections measured (7.046° ≤ 2θ ≤ 55.01°), 20 994 unique (R_{int} = 0.0638) which were used in all calculations. The final R_1 was 0.0389 ($I > 2\sigma(I)$) and wR_2 was 0.0782 (all data).

Crystal data for $C_{49}H_{50}N_8O_{12}Zn_2$ (**2a**): M = 1073.71 g mol^{-1}, tetragonal, space group $I4/mmm$ (no. 139), a = 21.7570(4), c = 34.6535(11) Å, U = 16403.8(8) Å^3, Z = 8, T = 200 K, μ(CuK$_\alpha$) = 1.075 mm^{-1}, D_{calc} = 0.870 g cm^{-3}, 56 809 reflections measured (7.684° ≤ 2θ ≤ 140.112°), 3216 unique (R_{int} = 0.0540) which were used in all calculations. The final R_1 was 0.1169 ($I > 2\sigma(I)$) and wR_2 was 0.4342 (all data).

Crystal data for $C_{112}H_{92}N_{20}O_{20}Zn_4$ (**2b**): M = 2299.53 g mol^{-1}, triclinic, space group $P\bar{1}$ (no. 2), a = 18.532(2), b = 20.3541(15), c = 20.561(2) Å, α = 116.099(8), β = 112.218(10), γ = 97.506(7)°, U = 6022.4(11) Å^3, Z = 2, T = 150 K, μ(MoK$_\alpha$) = 0.858 mm^{-1}, D_{calc} = 1.268 g cm^{-3}, 24 223 reflections measured (5.992° ≤ 2θ ≤ 43.932°), 13 116 unique (R_{int} = 0.1069) which were used in all calculations. The final R_1 was 0.1463 ($I > 2\sigma(I)$) and wR_2 was 0.4158 (all data).

Crystal data for $C_{24}H_{21}N_5O_5Zn$ (**3**): M = 524.83 g mol^{-1}, orthorhombic, space group $P2_12_12_1$ (no. 19), a = 10.1440(1), b = 13.9760(1), c = 16.1920(2) Å, U = 2295.58(4) Å^3, Z = 4, T = 150 K, μ(MoK$_\alpha$) = 1.117 mm^{-1}, D_{calc} = 1.519 g cm^{-3}, 44 382 reflections measured (7.068° ≤ 2θ ≤ 54.992°), 5253 unique (R_{int} = 0.0685) which were used in all calculations. The final R_1 was 0.0282 ($I > 2\sigma(I)$) and wR_2 was 0.0679 (all data).

Crystal data for $C_{47}H_{39}N_9O_9Zn_2$ (**4**): M = 1004.61 g mol^{-1}, monoclinic, space group $P2_1/c$ (no. 14), a = 10.040(6) Å, b = 29.598(17) Å, c = 17.153(11) Å, β = 102.762(5)°, U = 4971(5) Å^3, Z = 4, T = 150 K, μ(synchrotron, λ = 0.6889 Å) = 0.948 mm^{-1}, D_{calc} = 1.342 g cm^{-3}, 29 660 reflections measured (4.404° ≤ 2θ ≤ 50°), 8676 unique (R_{int} = 0.0938) which were used in all calculations. The final R_1 was 0.0740 ($I > 2\sigma(I)$) and wR_2 was 0.2075 (all data).

Crystal data for $C_{40}H_{29}N_5O_9Zn_2$ (**5a**): M = 854.42 g mol^{-1}, triclinic, space group $P\bar{1}$ (no. 2), a = 8.1920(2), b = 16.4330(4), c = 16.4440(4)Å, α = 93.7140(10), β = 99.8220(10), γ = 99.8070(10)°, U = 2139.30(9) Å^3, Z = 2, T = 150 K, μ(MoK$_\alpha$) = 1.177 mm^{-1}, D_{calc} = 1.326 g cm^{-3}, 42 369 reflections measured (7.07° ≤ 2θ ≤ 55.124°), 9831 unique (R_{int} = 0.0719) which were used in all calculations. The final R_1 was 0.0488 ($I > 2\sigma(I)$) and wR_2 was 0.1493 (all data).

Crystal data for $C_{40}H_{29}N_5O_9Zn_2$ (**5b**): M = 854.42 g mol^{-1}, monoclinic, space group $P2_1/c$ (no. 14), a = 21.9269(10), b = 23.8222(11), c = 8.2020(2) Å, β = 96.821(3)°, U = 4254.0(3) Å^3, Z = 4, T = 150 K, μ(MoK$_\alpha$) = 1.184 mm^{-1}, D_{calc} = 1.334 g cm^{-3}, 74 335 reflections measured (6.574° ≤ 2θ ≤ 54.968°), 9743 unique (R_{int} = 0.0514) which were used in all calculations. The final R_1 was 0.0677 ($I > 2\sigma(I)$) and wR_2 was 0.1810 (all data).

The structures were solved using SHELXS[21a] and refined using full-matrix least squares in SHELXL[21b] using the OLEX-2 interface.[21c] Details of the final refinements are provided in the ESI.† Unless noted therein, all non-hydrogen atoms were refined anisotropically in the final least squares cycles, and hydrogen atoms were included at calculated positions. The search for solvent accessible voids in the structures and their analysis was performed using the SQUEEZE subroutine of PLATON.[22]

Results and discussion

In this study, the reaction of zinc(II) nitrate hexahydrate with Hdpp was undertaken in the presence of a variety of dicarboxylic acids in order to observe the influence of the co-ligand on the network structure adopted. The carboxylic acids used are shown in Fig. 1 alongside the structure of Hdpp. In the cases of 1,4-benzenedicarboxylic acid (H_2bdc), 1,3-benzenedicarboxylic acid (H_2mbdc) and 5-methyl-1,3-benzenedicarboxylic acid (H_2mbdc-Me), a single product was obtained regardless of the stoichiometry employed. For the two isomers of naphthalene dicarboxylic acid, the reaction mixtures contained more than one phase, regardless of the reaction conditions or stoichiometry employed. For 1,4-naphthalene dicarboxylic acid (H_2ndc-1,4), two separate compounds were identified (**2a** and **2b**), though both refinements suffered from poor data quality. For 2,6-naphthalene dicarboxylic acid (H_2ndc-2,6), data sets were collected on two sets of crystals which had different unit cells. However, in this case, the two structures (**5a** and **5b**) were shown to have similar gross structures, in contrast to observations with **2a** and **2b**.

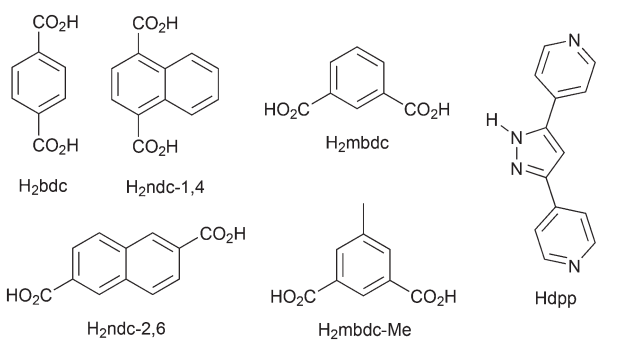

Fig. 1 The structures of Hdpp and the diacids used in this study.

$[Zn_2(bdc)_2(Hdpp)_2]\cdot 2DMF$ 1

The asymmetric unit of **1** consists of four zinc centres, four bdc ligands, four Hdpp ligands and four included DMF molecules. The compound adopts a structure based on $Zn_2(carboxylate)_4$ building blocks, though not the common paddlewheel motifs in which all four carboxylates bridge between the zinc(II) centres. Instead, two carboxylate groups bridge the zinc centres and the remaining two each bind single zinc centres in an asymmetric chelating mode ($d_{(Zn-O)}$ = 1.968(3)–2.063(3) Å, and 2.486(3)–2.979(3) Å for four unique contacts each). These secondary building units (SBUs) are linked into sheets by the benzene rings of the dicarboxylates (Fig. 2a). The Hdpp ligands coordinate in both axial positions on each zinc centre, and link each dimer into chains (Fig. 2b). Overall, these interactions serve to connect the zinc-bdc sheets into three-dimensional networks, which are doubly-interpenetrated (Fig. 2c). All of the pyrazole NH groups are involved in N–H···O hydrogen bonding – two form hydrogen bonds to those carboxylate oxygen atoms in the neighbouring framework that form the long coordination bonds [N(6)···O(16) 2.687(5), H(6)···O(16) 1.83 Å, N(6)–H(6)···O(16) 164°; N(14)···O(4) 2.752(5), H(14)···O(4) 1.94 Å, N(14)–H(14)···O(4) 153°] and these contacts link the interpenetrated frameworks together. The other two NH groups form hydrogen bonds with included DMF molecules [N(3)···O(19A) 2.66(4), H(3)···O(19A) 1.79 Å, N(3)–H(3)···O(19A) 171°; N(11)···O(17) 2.811(5), H(11A)···O(17) 1.96 Å, N(11)–H(11A)···O(17) 153°]. It is notable that both the SBU in **1** and the chains formed by linking the $Zn_2(carboxylate)_4$ dimers with the Hdpp ligands mirror similar structural features observed in $[Zn_2(OAc)_4(Hdpp)_2]\cdot MeOH$.[19]

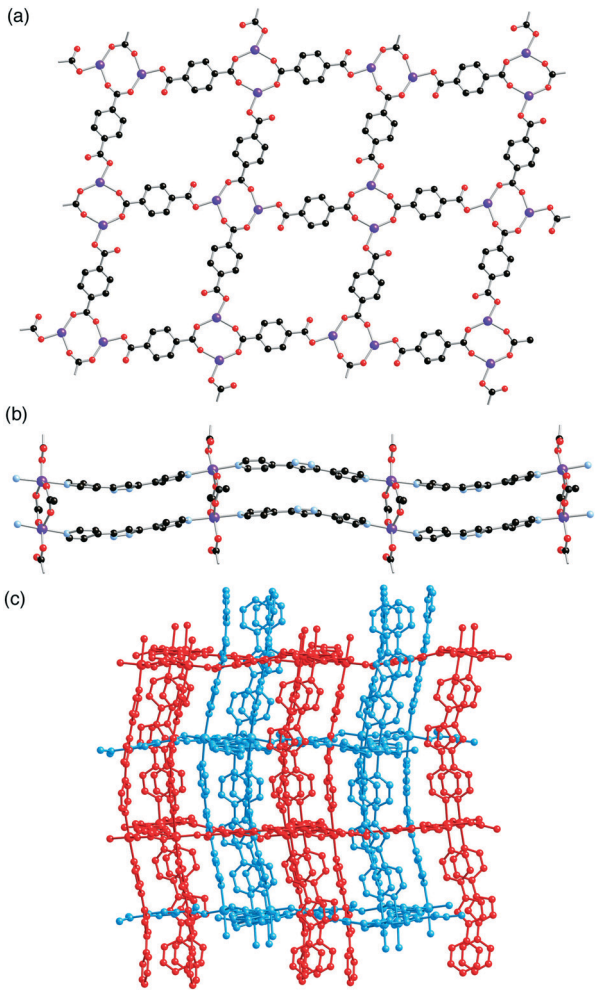

Fig. 2 The structure of $[Zn_2(bdc)_2(Hdpp)_2]\cdot 2DMF$ **1**, showing (a) the $Zn_2(bdc)_2$ sheets, (b) connecting the $Zn_2(O_2CR)_4$ SBUs into chains, and (c) the doubly-interpenetrated 3D structure.

The pair of Hdpp ligands bridging between pairs of SBUs are parallel to each other with the pyrazole carbon atoms 3.70 Å apart. While the Hdpp ligands are held together by coordination to the zinc centres, the relatively larger Zn···Zn separation of 3.95–3.97 Å suggests there may be π···π interactions between these ligands. Similar interactions are present in the crystal structure of $Hdpp\cdot 3H_2O$.[23]

A study of the Cambridge Structural Database (CSD) reveals that 38 structures containing zinc, bdc (or a substituted version) and bpy (or a substituted version) have been previously reported. Of these, only two – $[Zn_2(bdc)_2(bpy)_2]$ (LOTXOH)[24] and $[Zn_2\{bdc\text{-}(OH)_2\}_2(bpy)_2]$ (SUPLOF)[25] – form similar networks to **1** though, due to the shorter length of bpy with respect to Hdpp, these are non-interpenetrated. The most common structural type observed for zinc-bdc-bpy compounds has the general formula $[Zn_2(dicarboxylate)_2(bpy)]$ and consists of $Zn_2(carboxylate)_4$ paddlewheels that are linked into sheets by the benzene rings of the dicarboxylates, which are connected into three-dimensional networks by the bpy ligands. This is observed in 19 of the 38 structures, with the majority of these structures being interpenetrated. However, no evidence for a compound of the formula $[Zn_2(bdc)_2(Hdpp)]$ was observed in this study.

$[Zn_2(1,4\text{-}ndc)_2(Hdpp)]\cdot 4DMF$ 2a

The asymmetric unit of **2a** consists of half of a zinc centre, half an 1,4-ndc ligand and one half of a Hdpp linker at 50% occupancy, as well as some diffuse solvent. Interpretation of the X-ray data was hampered by symmetry issues which negatively impacted on the residuals that accompany the refinement (see ESI†), but unambiguous assignment of the framework was achieved.

Each pair of zinc(II) centres is bridged by four 1,4-ndc carboxylate groups, giving rise to the ubiquitous paddlewheel motif. In addition, each zinc(II) centre is coordinated to a pyridyl group from a Hdpp ligand. The bridging 1,4-ndc ligands correspondingly yield a (4,4) square net with paddlewheel nodes. The naphthalene group of each 1,4-ndc ligand is disordered over two positions. On average, each (4,4) 'square' adopts one of three conformations with regards to the naphthalene groups; in 50% of instances the opposing pairs of naphthalene groups are oriented both above and below the plane defined by the SBUs within each sheet, in 25%

of instances all of the naphthalene groups are oriented below this plane, and in the final 25% all are oriented above this plane (Fig. 3).

The bridging Hdpp ligands link the (4,4) nets formed from zinc(II) and 1,4-ndc, and the entire Hdpp ligand is disordered over two positions. Sterics play a dominant role in the structure of **2a**, with the bent nature of Hdpp influencing the orientation of the naphthalene groups within the 1,4-ndc sheets (Fig. 4). This provides justification for the pattern of naphthalene group ordering shown in Fig. 3. Interpenetration in **2a** is not observed, and it is likely that the steric bulk of the naphthalene moiety disfavours interpenetration within this type of framework. As a consequence of this, channels surround the Hdpp linkers. The poor quality of the diffraction data precluded assignment of the solvent, though this is modelled as one molecule of DMF per asymmetric unit on the basis of NMR analyses of the digested product.

[Zn(1,4-ndc)(Hdpp)]·DMF 2b

The asymmetric unit of **2b** consists of four zinc centres, four 1,4-ndc ligands and four Hdpp linkers, and some diffuse solvent modelled as one molecule of DMF per zinc(II) centre. The same issue regarding X-ray data quality applies in this case as for **2a**, though for **2b** the data were primarily compromised by a rapid decrease in intensity with increasing 2θ. In addition, evidence of a phase-transition from **2b** to **2a** was inferred for this material (see ESI†). As for **2a**, these deficiencies have affected the refinement residuals, which are higher than desirable. However, as for **2a**, the data do permit unambiguous assignment of the framework, and this dictates the limit of discussion herein.

Each zinc(II) centre is coordinated to two 1,4-ndc carboxylate groups and two Hdpp pyridyl groups. The metal centres therefore act as tetrahedral nodes, and the bridging ligands interlink them into three-dimensional diamondoid networks (Fig. 5a). The structure is fourfold-interpenetrated (Fig. 5b).

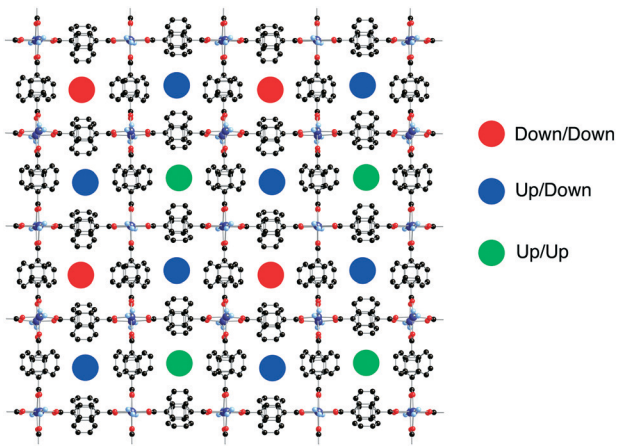

Fig. 3 The (4,4) net within $[Zn_2(1,4\text{-ndc})_2(Hdpp)]\cdot 4DMF$ **2a**, showing the orientation of the disordered naphthalene groups relative to the plane of the zinc-dicarboxylate sheets.

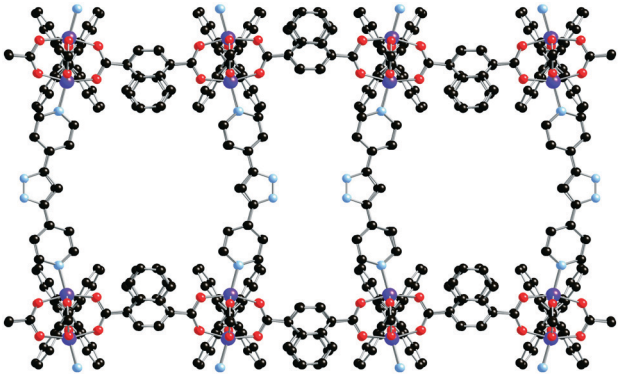

Fig. 4 The pillared layer structure of $[Zn_2(1,4\text{-ndc})_2(Hdpp)]\cdot 4DMF$ **2a** showing only one disordered component of the Hdpp linker, and with hydrogen atoms removed for clarity.

The relative proximity of pyrazole nitrogen atoms and carboxylate oxygen atoms suggests the presence of hydrogen bonding, which would interlink the networks in a pairwise manner.

1,4-Naphthalene dicarboxylate is a bulkier linker than 1,4-benzenedicarboxylate and it is likely that steric interactions

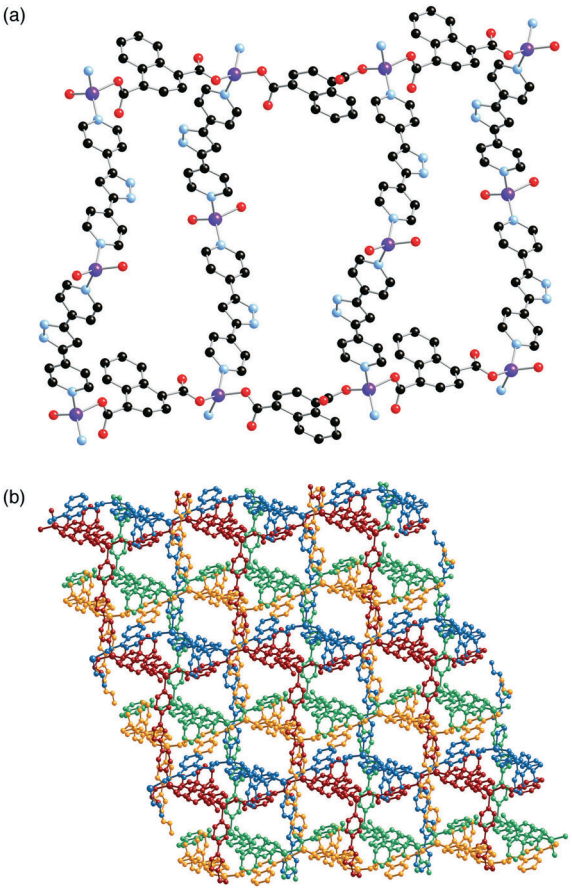

Fig. 5 The structure of [Zn(1,4-ndc)(Hdpp)]·DMF **2b**, showing (a) a portion of the diamondoid network, and (b) the fourfold interpenetration.

between the aromatic rings prevent the formation of a structure analogous to that of **1**. It is notable that none of the known zinc-bpy-dicarboxylate structures have a similar topology to **2b**, regardless of the observed ratio of the components.

Of the eight previously reported structures containing zinc(II), 1,4-ndc and bpy, five form the same structural type as **2a**. The compound [Zn(1,4-ndc)(H_2O)$_2$(bpy)] forms both open (XADFOZ) and closed (XOKVAV) layer structures,[26] whereas [Zn_2(1,4-ndc)$_2$(bpy)] (VIYZIO) adopts a structure in which Zn_2(carboxylate)$_4N_2$ nodes are linked into sheets by the naphthalene groups, and these sheets are inter-connected into an interpenetrated 3D structure by the bpy linkers.[27]

[Zn(mbdc)(Hdpp)]·DMF 3

The asymmetric unit of **3** consists of one zinc centre, one mbdc ligand, one Hdpp ligand and an included DMF molecule. The zinc(II) centre is coordinated to two mbdc carboxylate groups and two Hdpp pyridyl groups. The carboxylates are coordinated in an asymmetrical manner, with the longer contacts 2.497(2) Å and 2.813(2) Å, ensuring that the metal centres have distorted octahedral geometry but act as 4-connected nodes, bonding to two mbdc and two Hdpp ligands. These linking ligands connect the metal centres into two-dimensional networks with the (4,4) topology (Fig. 6).

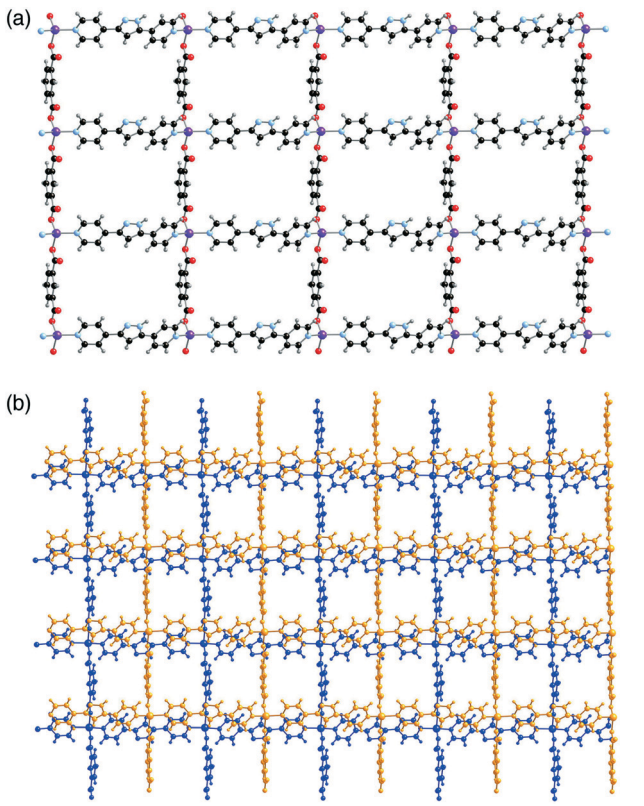

Fig. 6 The structure of [Zn(mbdc)(Hdpp)]·DMF **3**, showing (a) the 2D networks, and (b) pairs of 2D networks that are interlinked by hydrogen bonding.

The sheets are interlinked by hydrogen bonds involving the pyrazole fragment, with both N–H···O and C–H···O interactions present [N(3)···O(2) 2.710(3), H(3A)···O(2) 1.83 Å, N(3)–H(3A)···O(2) 174°; C(15)···O(3) 3.309(4), H(15)···O(3) 2.38 Å, C(15)–H(15)···O(3) 167°]. The N–H···O interaction involves the oxygen atom that forms the longer contact to the zinc centre, with the lengthening of this bond occurring concurrently with hydrogen bond formation that ensures that the sheets stack in a staggered manner.

A search of the Cambridge Structural Database revealed 49 crystal structures containing zinc, 1,3-benzenedicarboxylate and bpy (or substituted analogues). Of these, only two are isoreticular to **3**. In both [Zn(mbdc-NO_2)(bpy)] (UJOLUA, mbdc-NO_2 = 5-nitro-1,3-benzenedicarboxylate)[28] and [Zn(mbdc-pyr)(bpy)] (YATGOR, mbdc-pyr = 5-pyrrolinyl-1,3-benzenedicarboxylate)[29] the sheets also stack in a staggered fashion, with this facilitated by π···π stacking and, in the latter case, mutual interdigitation of the pyrrolinyl groups into the pores of a neighbouring sheet. The parallel mbdc ligands are too far apart in **3** for π···π stacking to occur (d > 6.6 Å), and the packing of the sheets provides cavities for the included disordered DMF molecules.

[Zn_2(mbdc-Me)$_2$(Hdpp)$_2$]·DMF 4

The asymmetric unit of **4** consists of two zinc centres, two mbdc-Me ligands, two Hdpp ligands and two half-occupancy DMF molecules, only one of which lent itself to being modelled in the refinement of the structural model. Compound **4** contains similar Zn_2(carboxylate)$_4$ SBUs to **1**, with two carboxylate groups bridging between the zinc centres and a carboxylate group asymmetrically coordinated to each zinc centre.

The 120° angle present between the carboxylate groups in the mbdc-Me ligand leads to the SBUs being connected into chains (Fig. 7a) rather than the sheets observed for **1**. Hdpp ligands coordinate in the axial positions of the zinc centres, and link the chains into sheets (Fig. 7b).

As in **1**, pairs of Hdpp ligands are brought into proximity by coordination to the zinc centres. There is evidence of π···π interactions between pairs of Hdpp ligands, with the closest distance between atoms in the parallel pyrazole rings (3.3 Å) considerably shorter than the Zn···Zn distance (4.0 Å). The pyrazole rings are also involved in inter-sheet interactions, with one of the independent ligands forming a N–H···O hydrogen bond to a carboxylate oxygen atom [N(6)···O(6) 2.781(5), H(6)···O(6) 1.91 Å, N(6)–H(6)···O(6) 173°]. The pyrazole ring on the second Hdpp linker forms a hydrogen bond with the included DMF molecule [N(3)···O(9) 2.745(8), H(3)···O(9) 1.89 Å, N(3)–H(3)···O(9) 162°].

The topology observed in **4** is similar to that observed in the CID class of MOFs reported by Kitagawa and coworkers,[30] and this structural type accounts for 13 of the 49 crystal structures present for zinc-bpy compounds with 1,3-benzene dicarboxylates in the CSD. These MOFs are of particular note for their flexibility, which is facilitated by the

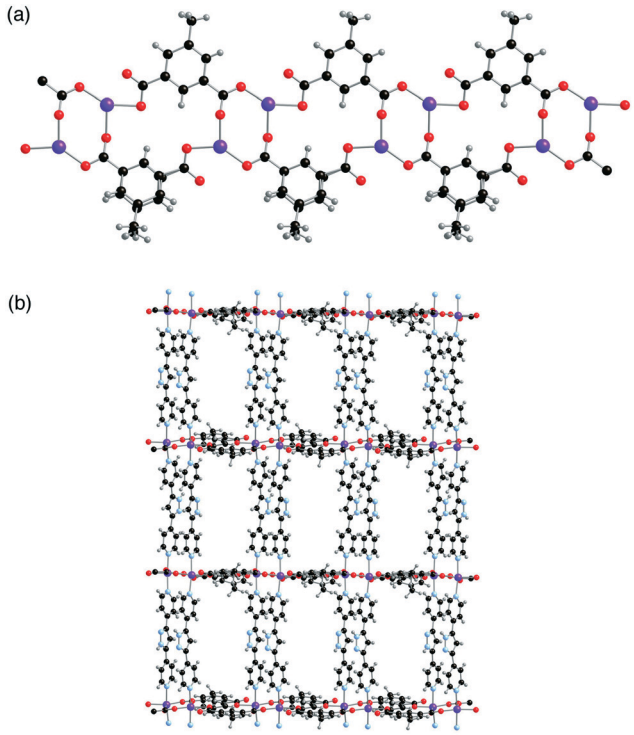

Fig. 7 The structure of $[Zn_2(mbdc\text{-}Me)_2(Hdpp)_2]\cdot DMF$ **4**, showing (a) the $Zn_2(mbdc\text{-}Me)_2$ tapes, and (b) the 2D network formed by interlinking the tapes with Hdpp ligands.

movement of neighbouring sheets with respect to each other.[31]

$[Zn_2(2,6\text{-}ndc)_2(Hdpp)]\cdot DMF$ 5a/5b

The asymmetric unit of **5a** consists of two zinc centres, one and two halves of 2,6-ndc ligands, one Hdpp ligand and a disordered DMF molecule. Each zinc centre is coordinated to three carboxylates and one Hdpp ligand. The full and partial occupancy 2,6-ndc ligands play very different structural roles. The two carboxylate groups in the linker containing O(1)–O(4) bridge between metal centres connecting them into zinc-carboxylate chains, which are linked into pairs by the naphthalene groups (Fig. 8a). π···π interactions are also present between the naphthalene rings, with a closest distance between atoms in neighbouring rings being 3.3 Å. The 2,6-ndc linkers containing O(5)–O(8) connect the pairs of chains into a three-dimensional network, which is further supported by the Hdpp ligands, which bridge zinc centres (Fig. 8b). The gross structure of **5b** is very similar to that of **5a** despite occupying a higher symmetry space group ($P2_1/c$ for **5b**, $P\bar{1}$ for **5a**).

The NH groups of the Hdpp ligands are not involved in hydrogen bond interactions to the carboxylate oxygen atoms, and project into the void space occupied by disordered DMF molecules. There is, however, stacking of the Hdpp ligands, with the closest distance between atoms being 3.4 Å.

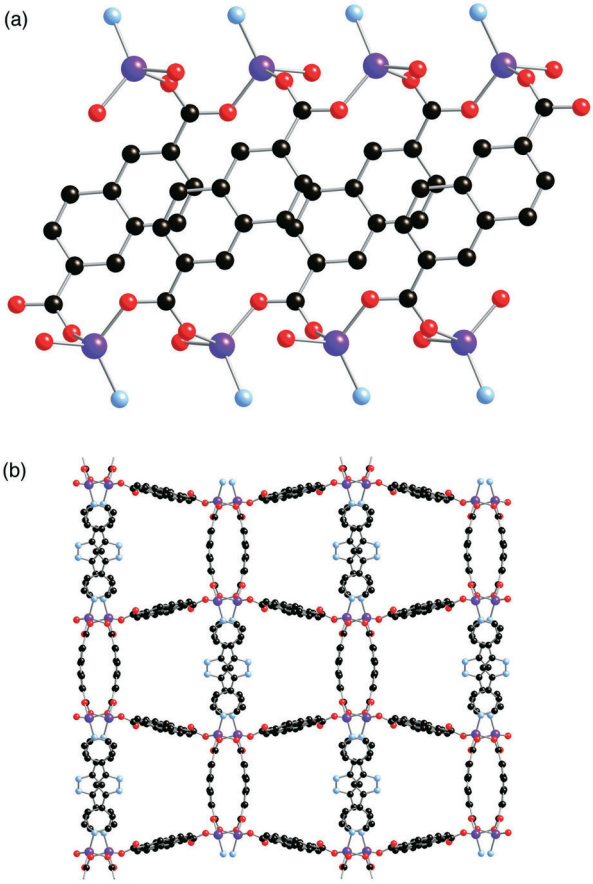

Fig. 8 The structure of $[Zn_2(2,6\text{-}ndc)_2(Hdpp)]\cdot DMF$ **5a**, showing (a) the tapes formed by linking zinc-carboxylate chains with 2,6-ndc ligands, and (b) the 3D network formed by interlinking the tapes with 2,6-ndc and Hdpp ligands.

There are eight previously reported structures containing zinc, 2,6-ndc and bpy (or a substituted analogue) instead of Hdpp. All adopt very different structures to **5a**, with zinc-2,6-ndc sheets linked into doubly- or triply-interpenetrated three-dimensional networks by the bpy linkers.[32]

Discussion

This research programme set out to evaluate how changing from bpy to Hdpp influences the nature of the zinc MOF products that contain both dicarboxylate and *N*,*N*′-ditopic ligands. Hdpp differs from bpy in three ways – the distance between the nitrogen donors, the angle between the nitrogen donors and the presence of hydrogen bonding groups in the pyrazole ring of the Hdpp ligand.

Insight into the importance of these factors can be acquired by comparing the structures of the new compounds **1**–**5** with those of their bpy analogues, as noted above, and compounds containing other *N*,*N*′-ditopic linkers. Structures involving 1,4-di(4-pyridyl)benzene (dpb) are particularly informative, given the similar length of the Hdpp and dpb ligands. Seven crystal structures containing zinc, bdc and either dpb or a substituted analogue have been reported. Five

of these form doubly-interpenetrated DMOF-1 type structures, whereas the other two form structures with a similar topology, but possess a different arrangement of the carboxylate groups around the zinc paddlewheel unit. These seven Zn-bdc-dpb structures all differ from those adopted by **1** and **2b**, but are similar to that of **2a**, demonstrating that the distortion from linearity of Hdpp does not prevent it from forming analogous structures to those with linear linkers. The zinc-bdc sheets present in **1** are less accessible to 1,4-ndc due to unfavourable steric interactions that would be present with the bulkier dicarboxylate.

Eight crystal structures containing zinc, mbdc and dpb or substituted analogues of these ligands have been reported. Two of these compounds are isoreticular with **4**, while four of the others adopt three-dimensional networks based on zinc-dicarboxylate sheets that are topologically similar to those present in **1**.

In four of the seven new structures reported in this paper, hydrogen bonding between the NH group in the pyrazole ring in the centre of the Hdpp ligand and a carboxylate oxygen serves to connect either interpenetrated three-dimensional networks or interdigitated two-dimensional networks together. The exceptions to this are **2a** and **5a**, **b**, for which the NH groups project into pores occupied by disordered solvent molecules.

Conclusions

We have shown that di(4-pyridyl)-1*H*-pyrazole (Hdpp) can act as a *N*,*N*′-ditopic co-linker in zinc dicarboxylate MOFs. X-ray structural analyses reveal that reaction of $Zn(NO_3)_2{\cdot}6H_2O$ with Hdpp in the presence of a dicarboxylic acid forms the compounds $[Zn_2(bdc)_2(Hdpp)_2]{\cdot}2DMF$ **1**, $[Zn_2(1,4\text{-ndc})_2(Hdpp)]{\cdot}4DMF$ **2a**, $[Zn(1,4\text{-ndc})(Hdpp)]{\cdot}DMF$ **2b**, $[Zn(mbdc)(Hdpp)]{\cdot}DMF$ **3**, $[Zn_2(mbdc\text{-}Me)_2(Hdpp)_2]{\cdot}DMF$ **4** and $[Zn_2(2,6\text{-ndc})_2(Hdpp)]{\cdot}DMF$ **5a**, **b**. In some cases, the products are isoreticular with those adopted by linear *N*,*N*′-ditopic ligands such as bpy and dpb, but the presence of the pyrazole group provides a means to interlink interpenetrated or interdigitated networks by hydrogen bonding. However, the structures of **2a** and **5a**, **b** reveals that this is not inevitable, as in these cases the hydrogen bonding groups project into the pores and are available to interact with guest molecules. Current research is focussed on the interactions of these frameworks with guest molecules and exploiting these interactions for selective separations.

Conflicts of interest

There are no conflicts to declare.

Acknowledgements

We thank the EPSRC (EP/K004956/1, EP/F007620/1) and the Leverhulme Trust for financial support.

Notes and references

1 (*a*) H. Furukawa, K. E. Cordova, M. O'Keeffe and O. M. Yaghi, *Science*, 2013, **341**, 1230444; (*b*) M. L. Foo, R. Matsuda and S. Kitagawa, *Chem. Mater.*, 2014, **26**, 310; (*c*) Y. Cui, B. Li, H. He, W. Zhou, B. Chen and G. Qian, *Acc. Chem. Res.*, 2016, **49**, 483.

2 (*a*) M. P. Suh, H. J. Park, T. K. Prasad and D.-W. Lim, *Chem. Rev.*, 2012, **112**, 782; (*b*) H. Wang, Q.-L. Zhu, R. Zou and Q. Wu, *Chem*, 2017, **2**, 52; (*c*) Y. Lin, C. Kong, Q. Zhang and L. Chen, *Adv. Energy Mater.*, 2017, **7**, 1601296.

3 (*a*) *Metal Organic Frameworks as Heterogeneous Catalysts*, ed. F. X. Llabrés, I Xamena and J. Gascon, RSC Catalysis Series, RSC Publishing, Cambridge, UK, 2013; (*b*) I. Nath, J. Chakraborty and F. Verpoort, *Chem. Soc. Rev.*, 2016, **45**, 4127; (*c*) M. Rimoldi, A. J. Howarth, M. R. DeStefano, L. Lin, S. Goswami, P. Li, J. T. Hupp and O. K. Farha, *ACS Catal.*, 2017, **7**, 997.

4 (*a*) J.-R. Li, J. Sculley and H.-C. Zhou, *Chem. Rev.*, 2012, **112**, 869; (*b*) R. Krishna, *RSC Adv.*, 2015, **5**, 52269.

5 (*a*) J. Zhang, S. Yao, S. Liu, B. Liu, X. Sun, B. Zheng, G. Li, Y. Li, Q. Huo and Y. Liu, *Cryst. Growth Des.*, 2017, **17**, 2131; (*b*) B. Li, M. Chrzanowski, Y. Zhang and S. Ma, *Coord. Chem. Rev.*, 2016, **307**, 106; (*c*) C. H. Hendon, F. Pradaux-Caggiano, L. E. Hatcher, W. J. Gee, C. C. Wilson, K. T. Butler, D. R. Carbery, A. Walsh and B. C. Melot, *Phys. Chem. Chem. Phys.*, 2016, **18**, 33329; (*d*) E. Madrid, M. A. Buckingham, J. M. Stone, A. T. Rogers, W. J. Gee, A. D. Burrows, P. R. Raithby, V. Celorrio, D. J. Fermin and F. Marken, *Chem. Commun.*, 2016, **52**, 2792.

6 (*a*) W. Lu, Z. Wei, Z.-Y. Gu, T.-F. Liu, J. Park, J. Park, J. Tian, M. Zhang, Q. Zhang, T. Gentle III, M. Bosch and H.-C. Zhou, *Chem. Soc. Rev.*, 2014, **43**, 5561; (*b*) W. J. Gee and S. R. Batten, *Cryst. Growth Des.*, 2013, **13**, 2335.

7 (*a*) K. K. Tanabe and S. M. Cohen, *Chem. Soc. Rev.*, 2011, **40**, 498; (*b*) W. J. Gee, L. K. Cadman, H. Amer Hamzah, M. F. Mahon, P. R. Raithby and A. D. Burrows, *Inorg. Chem.*, 2016, **55**, 10839; (*c*) A. D. Burrows, Post-synthetic modification of MOFs in ref. 3, p. 31.

8 M. Eddaoudi, J. Kim, N. Rosi, D. Vodak, J. Wachter, M. O'Keeffe and O. M. Yaghi, *Science*, 2002, **295**, 469.

9 (*a*) D. N. Dybtsev, H. Chun and K. Kim, *Angew. Chem., Int. Ed.*, 2004, **43**, 5033; (*b*) H. Chun, D. N. Dybtsev, H. Kim and K. Kim, *Chem. – Eur. J.*, 2005, **11**, 3521.

10 B. Chen, C. Liang, J. Yang, D. S. Contreras, Y. L. Clancy, E. B. Lobkovsky, O. M. Yaghi and S. Dai, *Angew. Chem., Int. Ed.*, 2006, **45**, 1390.

11 (*a*) D. Tanaka, A. Henke, K. Albrecht, M. Moeller, K. Nakagawa, S. Kitagawa and J. Groll, *Nat. Chem.*, 2010, **2**, 410; (*b*) S. Horike, D. Tanaka, K. Nakagawa and S. Kitagawa, *Chem. Commun.*, 2007, 3395.

12 (*a*) H. Chun, D. Dybtsev, H. Kim and K. Kim, *Chem. – Eur. J.*, 2005, **11**, 3521; (*b*) D. Ma, Y. Li and Z. Li, *Chem. Commun.*, 2011, **47**, 7377; (*c*) X. Zhang, L. Hou, B. Liu, L. Cui, Y.-Y. Wang and B. Wu, *Cryst. Growth Des.*, 2013, **13**, 3177; (*d*) W.-Y. Yin, Z.-L. Huang, X.-Y. Tang, J. Wang, H.-J. Cheng,

Y.-S. Ma, R.-X. Yuan and D. Liu, *New J. Chem.*, 2015, **39**, 7130.

13 T. Gadzikwa, O. K. Farha, C. D. Malliakas, M. G. Kanatzidis, J. T. Hupp and S. T. Nguyen, *J. Am. Chem. Soc.*, 2009, **131**, 13613.

14 (*a*) K. L. Mulfort and J. T. Hupp, *J. Am. Chem. Soc.*, 2007, **129**, 9604; (*b*) B.-Q. Ma, K. L. Mulfort and J. T. Hupp, *Inorg. Chem.*, 2005, **44**, 4912.

15 O. K. Farha, C. D. Malliakas, M. G. Kanatzidis and J. T. Hupp, *J. Am. Chem. Soc.*, 2010, **132**, 950.

16 S.-H. Cho, B. Ma, S. T. Nguyen, J. T. Hupp and T. E. Albrecht-Schmitt, *Chem. Commun.*, 2006, 2563.

17 W. Bury, D. Fairen-Jimenez, M. B. Lalonde, R. Q. Snurr, O. K. Farha and J. T. Hupp, *Chem. Mater.*, 2013, **25**, 739.

18 (*a*) H. J. Park, Y. E. Cheon and M. P. Suh, *Chem. – Eur. J.*, 2010, **16**, 11662; (*b*) L. Sbircea, N. D. Sharma, W. Clegg, R. W. Harrington, P. N. Horton, M. B. Hursthouse, D. C. Apperley, D. R. Boyd and S. L. James, *Chem. Commun.*, 2008, 5538.

19 A. D. Burrows, D. J. Kelly, M. I. Haja Mohideen, M. F. Mahon, V. M. Pop and C. Richardson, *CrystEngComm*, 2011, **13**, 1676.

20 V. N. Nuriev, N. V. Zyk and S. Z. Vatsadze, *ARKIVOC*, 2005, 208.

21 (*a*) G. M. Sheldrick, *Acta Crystallogr., Sect. A: Found. Crystallogr.*, 2008, **64**, 112; (*b*) G. M. Sheldrick, *Acta Crystallogr., Sect. A: Found. Adv.*, 2015, **71**, 3; (*c*) O. V. Dolomanov, L. J. Bourhis, R. J. Gildea, J. A. K. Howard and H. Puschmann, *J. Appl. Crystallogr.*, 2009, **42**, 339.

22 A. L. Spek, *Acta Crystallogr., Sect. D: Biol. Crystallogr.*, 2009, **65**, 148.

23 S.-Z. Zhan, D. Li, X.-P. Zhou and X.-H. Zhou, *Inorg. Chem.*, 2006, **45**, 9163.

24 J. Tao, M.-L. Tong and X.-M. Chen, *J. Chem. Soc., Dalton Trans.*, 2000, 3669.

25 T. Yamada and H. Kitagawa, *J. Am. Chem. Soc.*, 2009, **131**, 6312.

26 (*a*) P. Kanoo and T. K. Maji, *Eur. J. Inorg. Chem.*, 2010, 3762; (*b*) H.-P. Xiao, S. Aghabeygi, Z. Wei-Bing, Y.-Q. Cheng, W.-Y. Chen, J. Wang and A. Morsali, *J. Coord. Chem.*, 2008, **61**, 3679.

27 D.-Y. Ma, H.-F. Guo, L. Qin, Y. Li, Q.-T. Ruan, Y.-W. Huang and J. Xu, *J. Chem. Crystallogr.*, 2014, **44**, 63.

28 J. Tao, X. Yin, Y.-B. Jiang, L.-F. Yang, R.-B. Huang and L.-S. Zheng, *Eur. J. Inorg. Chem.*, 2003, 2678.

29 M. Yang, H.-J. He, F.-P. Zhai, X.-F. Liu, L.-H. Weng and Y.-M. Zhou, *Chin. J. Struct. Chem.*, 2012, **31**, 51.

30 D. Tanaka, A. Henke, K. Albrecht, M. Moeller, K. Nakagawa, S. Kitagawa and J. Groll, *Nat. Chem.*, 2010, **2**, 410.

31 A. Schneemann, V. Bon, I. Schwedler, I. Senkovska, S. Kaskel and R. A. Fischer, *Chem. Soc. Rev.*, 2014, **43**, 6062.

32 H. Aggarwal, P. M. Bhatt, C. X. Bezuidenhout and L. J. Barbour, *J. Am. Chem. Soc.*, 2014, **136**, 3776.